Journal of the European Ceramic Society 17 (1997) 905–911

PII: S0955-2219(96)00201-4
0955-2219/97/$17.00

Wet and Salt Corrosion of a Porous Si_2N_2O–ZrO_2 Composite Material

Maiken Heim,[a] Jiaxin Chen[a] & Robert Pompe[b]

[a]Department of Inorganic Chemistry, Chalmers University of Technology and Göteborg University, S-412 96 Göteborg, Sweden
[b]Swedish Ceramic Institute, Box 5403, S-402 29 Göteborg, Sweden

(Received 22 July 1996; revised version received 13 September 1996; accepted 23 September 1996)

Abstract

The hot corrosion behaviour of a low-cost, porous Si_2N_2O–ZrO_2 composite material, fabricated without the use of sintering additives has been studied in pure oxygen, humid oxygen (10, 15 and 20 vol% H_2O) and salt-containing environment (25 ± 5 ppm (in volume) NaCl). The corrosion experiments were carried out at 1000, 1200 and 1400°C.

For salt corrosion, a special test rig was used to simulate salt-containing combustion environments. The extent of internal oxidation has been found to be sensitive to the oxidation temperature. High oxidation resistance has been observed at temperatures >1200°C. Wet salt corrosion at temperatures above 1200°C shows no increased attack on the material.
© 1997 Elsevier Science Limited.

1 Introduction

Nitrogen ceramics have good oxidation, corrosion and thermal shock resistance. This makes them interesting for high temperature applications,[1] where the ceramics are exposed to harsh environments, which may contain excess oxygen, water vapour and salt species. One possible source of component failure in these applications is oxidative/corrosive degradation at high temperatures. It is therefore of great importance to elucidate the oxidation/corrosion mechanism of these ceramics.

In previous oxidation studies of the porous Si_2N_2O–ZrO_2 composite material[2–6] it was found that at temperatures up to 1250°C ZrO_2 is not significantly involved in the oxidation reaction and Si_2N_2O is oxidised to form a SiO_2 layer on both external and all internal surfaces. At higher temperatures, however, ZrO_2 reacts with SiO_2 to form a protective layer of zirconium silicate on all surfaces.

Humid environment (10 vol% $H_2O_{(g)}$) with or without 12 ppm salt has been found[6] to enhance oxidation and corrosion at temperatures ≤1250°C as compared to dry conditions. This enhancement is less profound at higher temperatures, which is probably caused by formation of a protective diffusion barrier containing zirconium silicate and cristobalite.

In this paper the short term oxidation/corrosion behaviour of the porous Si_2N_2O–ZrO_2 composite has been examined during the first 5 h of exposure in the following environments:

(a) O_2
(b) O_2 + H_2O (10, 15, 20 vol%)
(c) O_2 + NaCl (25 ± 5 ppm) + H_2O (0, 10, 15, 20 vol%).

The purpose of this study was to investigate the short-term corrosion behaviour of the composite material and the influence of oxidation and corrosion on the pore structure of the exposed samples.

2 Experimental

2.1 Material

The material examined in this work is an Si_2N_2O–ZrO_2 composite, fabricated by the nitrided, pressureless sintering technique (NPS) at the Swedish Ceramic Institute with Si and $ZrSiO_4$ as starting materials, according to eqn (1).[7,8]

$$3\,Si + ZrSiO_4 + 2N_2 \rightarrow 2\,Si_2N_2O + t\text{-} + m\text{-}ZrO_2 \quad (1)$$

(t tetragonal, m monoclinic)

The nominal phase composition of the sintered material is 64 wt% Si_2N_2O and 36 wt% ZrO_2. A residual $ZrSiO_4$ phase in the samples has also been detected. The material density was determined to be 3·05 ± 0·04 g/cm^3 with 15·0 ± 3·5% open porosity as determined by water intrusion

technique. The BET specific surface area of the as-received samples was 1·94 ± 0·03 m^2/g and the mean pore diameter, as measured by mercury intrusion method, was 0·08 μm.

2.2 Dry oxidation

The samples were oxidised in an alumina (99·7% purity) tube furnace in flowing dry oxygen with 4×10^{-3} m/s flow rate. The exposure temperatures were 1000, 1200 and 1400°C, respectively. The samples were intermittently taken out from the furnace, air cooled and weighed.

2.3 Oxidation in humid oxygen

Wet oxidation experiments were carried out in the above furnace connected to a steam generator. Oxygen gas was bubbled through boiling deionised water with a flow rate of 0·012 m/s. The saturated gas was then passed through a mantle heater which was connected to a thermostat. The bath temperatures were set corresponding to 10, 15 or 20 vol% H_2O. Water condensation before the gas entered the furnace was prevented by wiring those areas with heating wires thus keeping them at the temperature above the dew point. The same temperatures and times of exposure as in dry oxidation were used.

2.4 Salt corrosion in humid oxygen

A salt aerosol generator (Fig. 1),[9] was used to generate a low salt flux in the exposure environment. By dispersing a solution into air and evaporating the solvent, an aerosol of the solute is formed. The aerosol passes from the generator to a diffusion drier. The salt particles were then directly introduced into the hot zone of the furnace so as to avoid any serious interaction with water vapour. The salt concentration in the hot zone was determined to be 25 ± 5 ppm (by volume). The total gas flow rate was 0·012–0·017 m/s.

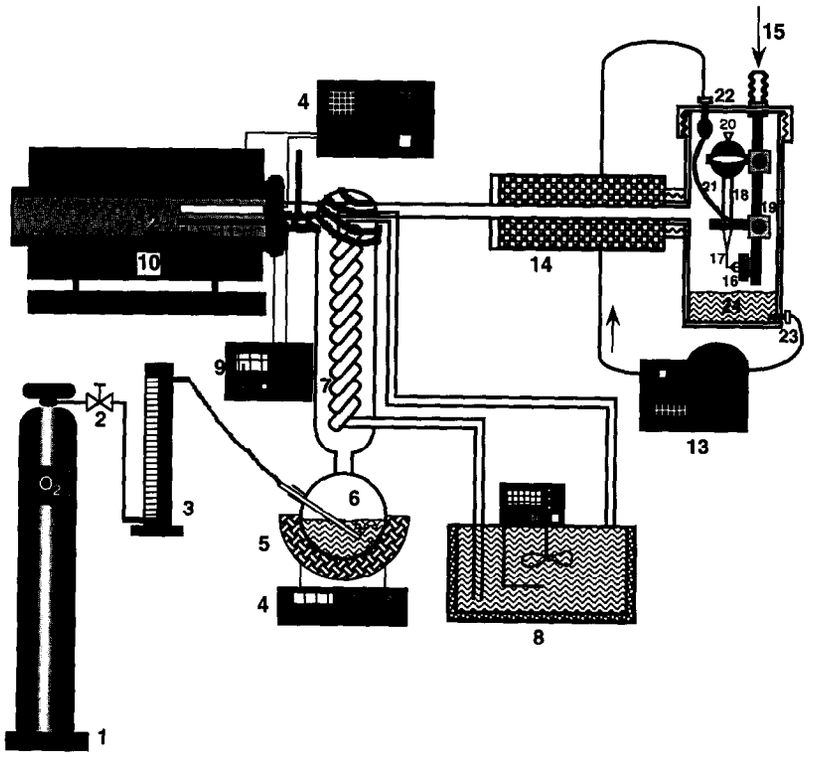

1	Gas supply	15	Pressurised air inlet
2	Needle valve	16	Glass capillary air flow regulator
3	Flow meter	17	90° tip hypodermic needle
4	Temperature controller	18	Flat spring allowing z-adjustment
5	Mantle heater	19	Mounting for z-adjustment screw and impaction buffle
6	Evaporator	20	x-adjustment screw (up-down)
7	Condenser	21	Liquid feed tubing
8	Thermostat	22	Filter for feed liquid
9	Ribbon heater	23	Liquid outlet to pump
10	Electric tube furnace	24	Liquid reservoir
11	Thermocouple		
12	Samples		
13	Peristaltic pump		
14	Diffusion drier		

Fig. 1. Experimental set-up with aerosol generator.

2.5 Calculation of porosity and weight gain

A number of methods for the calculation of the absolute permeability of porous media from pore level dimensions without invoking property-independent fitting parameters have been presented[11] to describe porous media, but they are in far from daily use in laboratory application.

For the calculation of the weight gain a cylindrical tube model was applied where the weight gain was related to the initial total surface area of the as-received material, according to eqn (2).

$$A_{tot_{t=0}} = A_{ext} + \frac{2P_0V_t}{r_0} \qquad (2)$$

where:

A_{tot} Total sample surface area
A_{ext} External surface area
P_0 Initial porosity
V_t Total volume of the sample
r_0 Initial pore radius

2.6 Thermodynamics of the exposure environments

To examine the high-temperature equilibrium composition of the gas mixtures used in the present studies, thermodynamic calculations were carried out using the SOLGASMIX computer program.[10]

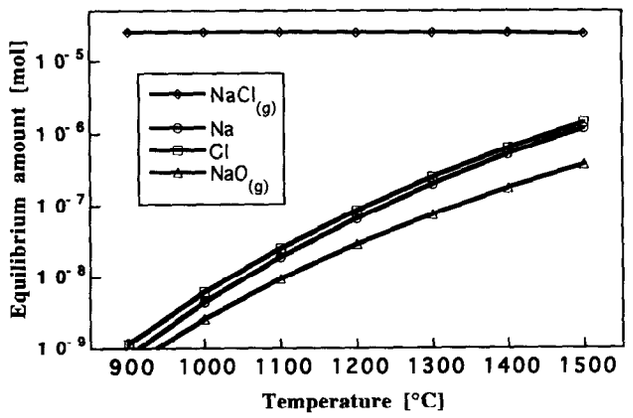

Fig. 2. Equilibrium compositions versus temperature curves for the input mixtures O_2–NaCl. The input amounts are 1 mol O_2 and $2{\cdot}5 \times 10^{-5}$ mol NaCl.

3 Results

3.1 Thermodynamics of the exposure environments

Figures 2 and 3 show the temperature dependence of the equilibrium composition of the input mixtures of O_2–NaCl and O_2–NaCl–H_2O in the temperature range 900–1500°C. Gaseous species whose amounts are less than 10^{-9} mol are not shown in the figures. The amounts of O_2 and H_2O remain approximately the same as the input amounts and are not shown in the figure.

In the wet oxidation environment the possible species thus are O_2, H_2O and trace H and H_2. The equilibrium concentrations of H and H_2 increase with temperature.

In dry salt corrosion environment, O_2, trace NaO, atomic Na and Cl form. The equilibrium concentrations of atomic Na and Cl and NaO increase with temperature.

In wet salt corrosion environment the equilibrium concentration of $NaCl_{(g)}$ decreases with temperature while $NaOH_{(g)}$ and $HCl_{(g)}$ increase. The formation of $NaOH_{(g)}$ and $HCl_{(g)}$ is favoured by increasing water concentration (not shown). Trace amounts of $NaO_{(g)}$, $H_{2(g)}$ and atomic Na, Cl, and H may also form.

3.2 Oxidation and corrosion kinetics

The reproducibility error of the weight change measurements was within $\pm 0{\cdot}3$ $\mu g/cm^2$.

3.2.1 Wet oxidation

At 1200°C, the final weight gain level decreases with increasing humidity, as shown in Fig. 4. As shown earlier,[2–6] the weight gain during dry oxidation ceases to increase after 5–20 h exposure.

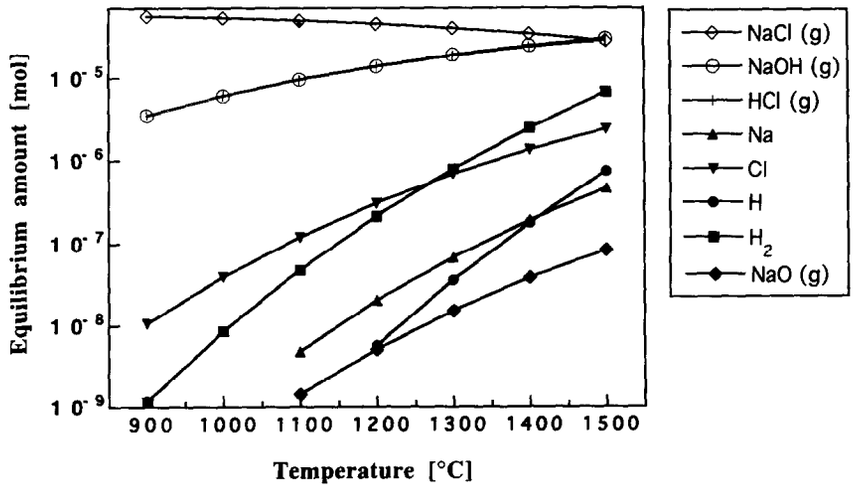

Fig. 3. Equilibrium composition versus temperature curves for the input mixture O_2–NaCl–H_2O. Input amounts: 0·85 mol O_2, 0·15 mol H_2O and $2{\cdot}5 \times 10^{-5}$ mol NaCl.

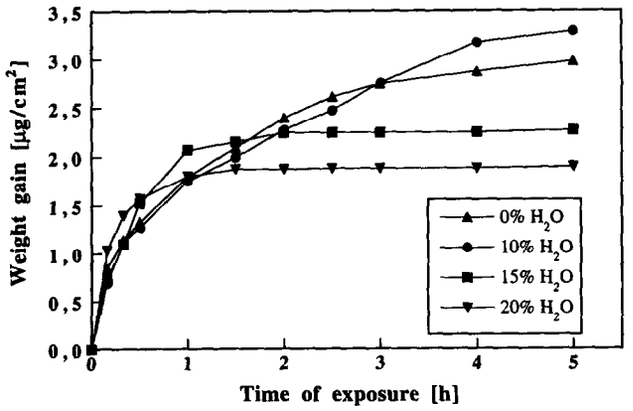

Fig. 4. Weight gain obtained during wet oxidation at 1200°C.

As can be seen from Fig. 4 the final weight gain at 1200°C decreases with increasing amount of water vapour.

A comparison of the final weight gain obtained after 5 h exposure in humid oxygen is summarised in Fig. 5. It can be seen that at 1000°C the general trend during wet oxidation is an increase of final weight gain with increasing water partial pressure. The opposite effect is observed at 1200 and 1400°C, where after the rapid initial oxidation the final weight gain decreases with increasing water partial pressure. This effect is less profound at 1400°C than at 1200°C.

3.2.2 Dry salt corrosion

Figure 6 shows a comparison of weight gain curves for dry salt corrosion compared to these for dry oxidation. Compared to dry oxidation, dry salt corrosion seems to be enhanced at 1000°C for the entire exposure period, while at 1200°C after rapid initial weight gain, the final weight gain is only about half of that after dry oxidation. At 1400°C, however, little difference in weight gain is seen.

3.2.3 Wet salt corrosion

At 15 and 20% humidity the curves bend down after rapid initial weight gain. It is observed that

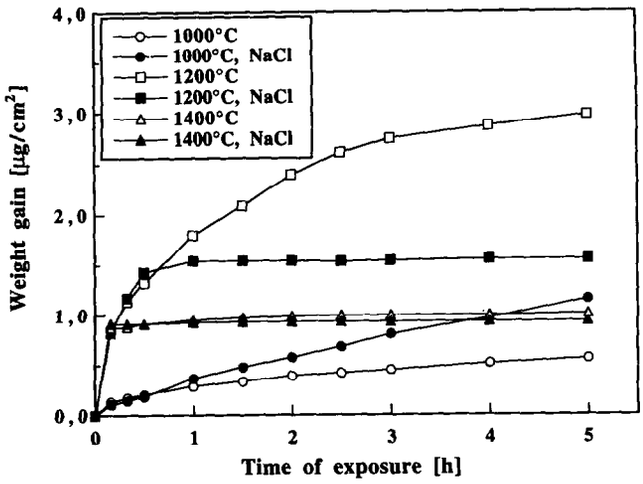

Fig. 6. Weight gain versus time of exposure curves during dry oxidation and dry salt corrosion at various temperatures.

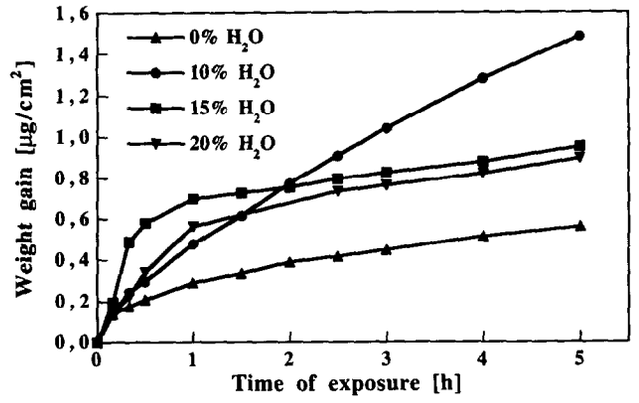

Fig. 7. Weight gain versus time of exposure curves at various water vapour contents during wet salt corrosion at 1000°C.

for all curves the weight gains continue even after 5 h of exposure (not shown). At 1200°C all final weight gains for wet salt corrosion are smaller than those for wet oxidation. The weight gains reach their maximum after about 1 h and remain approximately unchanged during the extended exposure (Fig. 8). At 1400°C the weight remains approximately unchanged after the first 10 min of exposure, which is similar to that occurring in wet oxidation, and no significant difference in weight

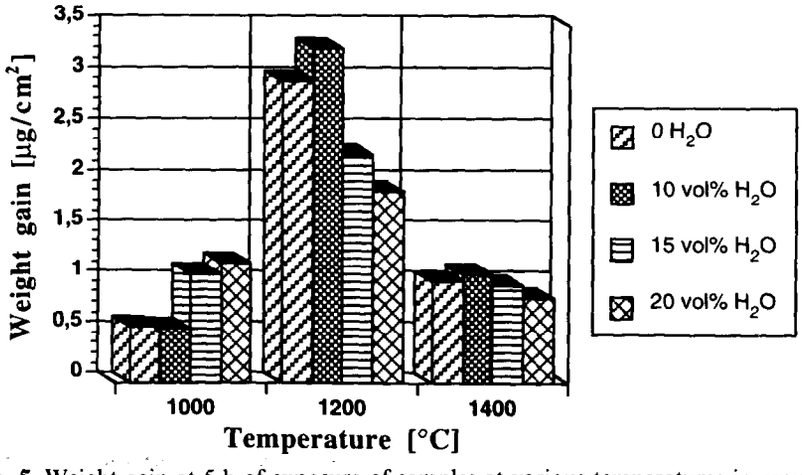

Fig. 5. Weight gain at 5 h of exposure of samples at various temperatures in oxygen.

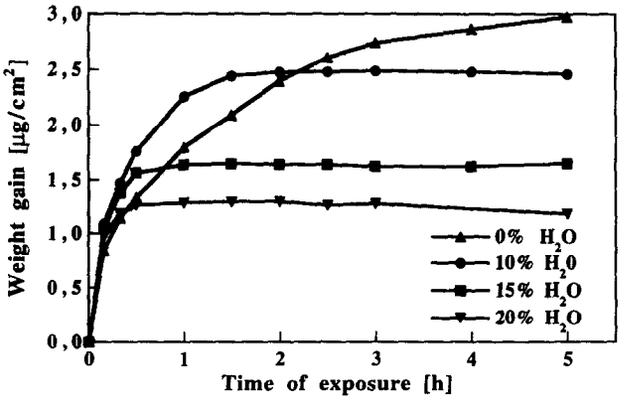

Fig. 8. Weight gain versus time of exposure curves at various water vapour contents during wet salt corrosion at 1200°C.

gain was observed for all kinds of exposure at this temperature.

A comparison of the final weight gains obtained after 5 h exposure during wet salt corrosion is given in Fig. 9. At all temperatures it is seen that with increase of the water partial pressure the final weight gain decreases. This observation seems to be independent of the initial open porosity.

3.3 Open porosity

Figure 10 summarises the changes in relative open porosity after exposures at 1000, 1200 and 1400°C in different environments. At 1000°C, the relative open porosity only changes approximately 0–20%. In particular, during wet salt corrosion little change is seen in open porosity before and after exposure. At 1200°C a significant decrease in open porosity is seen in wet corrosion and dry salt corrosion. At 15 and 20% water vapour content, wet corrosion leads to smaller open porosity than wet salt corrosion. At 1400°C it can be clearly seen that wet salt corrosion affects the open porosity to a lesser extent than wet oxidation does.

3.4 Phase analysis of corroded samples

XRD phase analysis of the sample surface shows that at temperatures ≥1200°C $ZrSiO_4$ is formed.

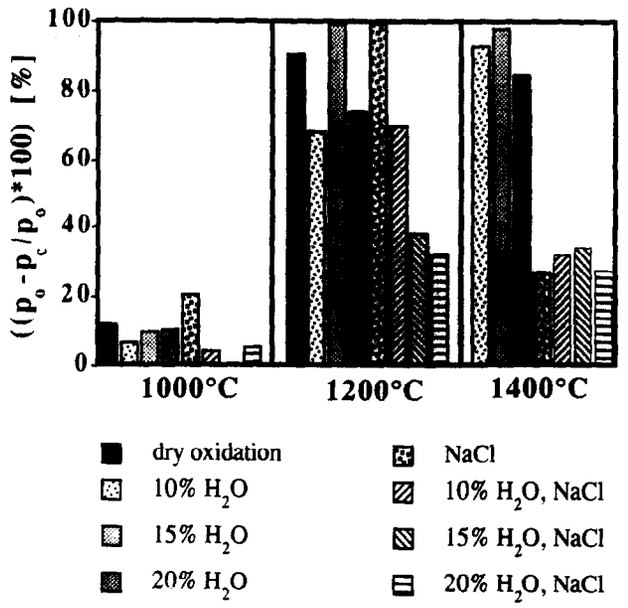

Fig. 10. Open porosity changes for samples exposed for 5 h to different environments (p_0 is the open porosity of as-received samples and p_c is the open porosity after exposure).

3.4.1 Wet oxidation

During wet oxidation, with increasing temperature *m*-ZrO_2 decreases, the *t*- (and/or *t'*-) ZrO_2 (up to 1200°C) and $ZrSiO_4$ content increases. The profound formation of cristobalite takes place only at 1400°C.

3.4.2 Wet salt corrosion

During wet salt corrosion only at 1000°C *m*-ZrO_2 was detected. Cristobalite was seen to decrease with increasing temperature.

4 Discussion

The general feature of oxidation weight gain versus time curves of this composite[3,5] is that, above a certain temperature (1100°C) the increase in the initial oxidation rate by, for instance, increased temperature is usually followed by decreased final weight gains. (Scattering in weight gain is probably mostly due to the differences in the initial open

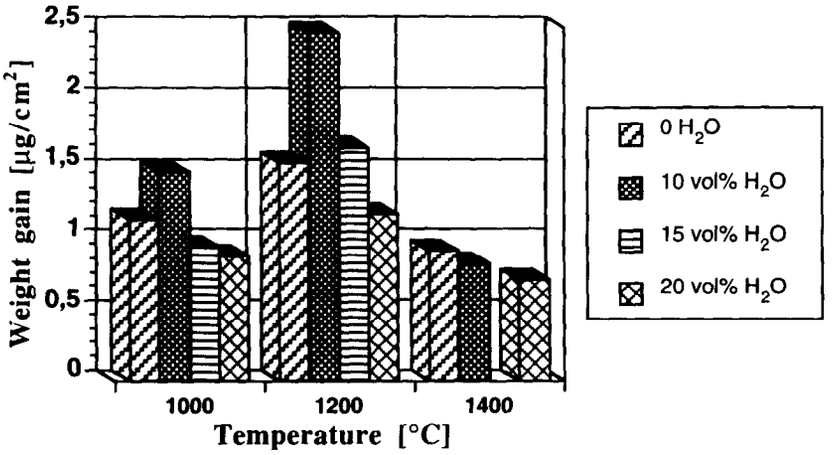

Fig. 9. Weight gain during wet salt corrosion after 5 h as a function of temperature and water vapour content.

porosity of different samples.) In the case of reaction bonded silicon nitride the similar effect is explained as due to pore sealing by the oxidant at the sample surface at higher temperatures and thereby the decrease of the accessible total surface area.

4.1 Effect of water vapour

The fact that the weight gain during wet oxidation is generally higher than during dry oxidation, suggests H_2O being the most oxidising species present in the gaseous environment. With increasing partial pressure of water vapour, at 1000°C and 1200°C the initial oxidation rates are seen to increase (Fig. 11). At 1200°C the formation of silica, which reduces the initial open porosity significantly (Fig. 10), seems to be greatly enhanced by water vapour causing extensive pore sealing, and inhibits further oxidation. The final weight gain is thus seen to decrease with increasing water vapour pressure.

During wet oxidation at 1400°C significant reduction of the open porosity occurs, implying that extensive surface pore sealing has occurred. The extensive pore sealing during wet oxidation at temperatures ≥1200°C complicates the exact calculation of the weight gain per unit area as the total surface area (both external and internal) decreases drastically with time.

4.2 Effect of NaCl

4.2.1 Dry salt corrosion

Under the salt corrosion conditions, $NaCl_{(g)}$ and $NaO_{(g)}$ may be present in the environment. NaCl is not sufficiently basic to dissolve the SiO_2 which forms on the surface of Si-based ceramics, while NaO may react with the SiO_2 to become the glass network modifier thereby increasing the diffusivity of oxygen in the scale. This may be the reason that in dry salt corrosion at 1000°C corrosion is considerably increased in the presence of salt (Fig. 6).

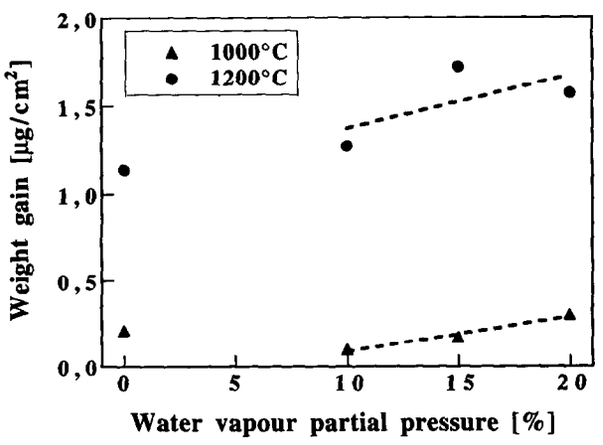

Fig. 11. Initial weight gain (0·5 h) versus partial pressure of water vapour at dlfferent temperatures.

At 1200°C higher initial weight gain (0·5 h in dry salt corrosion) leads to smaller final weight gain than that in dry oxidation, in which partial surface pore sealing occurs.[6] The sealing is enhanced significantly in the presence of salt, as the open porosity of the sample is close to zero. This might explain the reduced weight gain after about 1 h of exposure, because only the external surface is accessible now to the oxidant.

At 1400°C only a slight decrease in open porosity has been determined after dry salt corrosion and it seems that at this temperature the reaction of silica with ZrO_2 and subsequent formation of a $ZrSiO_4$-containing protective scale is a more important process in terms of protecting the material from further corrosion.

4.2.2 Wet salt corrosion

Under the wet salt corrosion conditions, mainly $NaCl_{(g)}$, $NaOH_{(g)}$, $HCl_{(g)}$, $H_{2(g)}$, $NaO_{(g)}$ and atomic H, Na and Cl might be present. NaOH can provide O^{2-} ions which combine with SiO_2 to form SiO_3^{2-} or SiO_4^{4-}, causing corrosive etching, or to increase the concentration of Na^+ in the glass structure. This may explain the accelerated corrosion of the material under the wet salt corrosion conditions at 1000°C.

At 1200°C, the lowest weight gain has been obtained during wet salt corrosion among all other treatments carried out at this temperature. This might be affected by the sodium-induced devitrification of the formed silica scale, which makes O_2 permeation difficult and therefore decreases the corrosion rate.

At 1400°C the initial oxidation rate is increased and the formation of $ZrSiO_4$ and SiO_2 is favoured in the presence of salt and the composite exhibits the best corrosion resistance. Among all kinds of corrosion, wet salt corrosion leads to the smallest changes in open porosity and pore sealing on the sample surface.

The experimental results presented show that the porous Si_2N_2O–ZrO_2 composite material can resist wet salt corrosion at high temperatures.

5 Conclusions

(1) A salt corrosion test rig has been constructed, which is capable of generating a continuous salt flux in the exposure environment.
(2) Corrosion resistance is considerably affected at 1000 and 1200°C when NaCl is introduced in a dry environment.
(3) Surface pore sealing, which is considerable during wet oxidation, is decreased by the presence of salt.

(4) The porous Si_2N_2O–ZrO_2 composite material exhibits good resistance to wet salt corrosion at high temperatures.

Acknowledgement

Financial support from the Swedish Board for Industrial and Technical Development (NUTEK) is gratefully acknowledged.

References

1. Hoggard, D. B., Park, H. K., Morrison, R. and Slasor, S., O'-Zirconia and its refractory applications. *Am. Ceram. Soc. Bull.*, 1990, **69**, 1163–1166.
2. Heim, M., Arwin, H., Chen, J. and Pompe, R., Determination of oxide thickness on an Si_2N_2O–ZrO_2 composite by spectroscopic ellipsometry. *J. Europ. Ceram. Soc.*, 1995, **15**(4), 313–318.
3. O'Meara, C., Heim, M. and Pompe, R., The oxidation of a porous Si_2N_2O–ZrO_2 composite material. *J. Europ. Ceram. Soc.*, 1995, **15**(4), 319–328.
4. Heim, M., Chen, J. and Pompe, R., Dry- and wet oxidation of an Si_2N_2O–ZrO_2 composite material. *J. Mat. Sci.*, (submitted).
5. Heim, M., Chen, J., Pompe, R. and Arwin, H., High temperature oxidation behaviour of an Si_2N_2O–ZrO_2 composite. In *Proc. of the 5th Intern. Symp. on Ceramic Materials & Components for Engines*, Shanghai, China, 1994, pp. 473–476.
6. Heim, M., Chen, J., O'Meara, C. and Pompe, R., The oxidation and salt corrosion of an Si_2N_2O–ZrO_2 composite material. *Ceram. Eng. & Sci. Proc.*, **17**(4, 5) 1996.
7. Pompe, R., US Patent No. 438 416, SE. Pat. No. 8702268-7, 1987.
8 Pompe, R., Patent Co4B 35/48, 35/58, 1988.
9. Lindqvist, O., Ljungström, E. and Svensson, R., Low temperature thermal oxidation of nitric oxide in polluted air. *Atmospheric Environment*, 1982, **16**, 1957–1972.
10. Eriksson, G., Thermodynamic studies of high temperature equilibria. *Chemica Scripta*, 1975, **8**, 100–103.
11. Matthews, G. P., Moss, A. K., Spearing, M. C. and Voland, F., Network calculation of mercury intrusion and absolute permeability in sandstone and other porous materials. *Powder Technology*, 1993, **76**, 95–107.